Gated Myocardial Perfusion SPECT: Basic Principles, Technical Aspects, and Clinical Applications

Asit K. Paul, MBBS, PhD; and Hani A. Nabi, MD, PhD

Department of Nuclear Medicine, State University of New York, University at Buffalo, Buffalo, New York

Electrocardiographically gated myocardial perfusion SPECT (GSPECT) is a state-of-the-art technique for the combined evaluation of myocardial perfusion and left ventricular function within a single study. It is currently one of the most commonly performed cardiology procedures in a nuclear medicine department. Automation of the image processing and quantification has made this technique highly reproducible, practical, and user friendly in the clinical setting. In patients with coronary artery disease, gating enhances the diagnostic and prognostic capability of myocardial perfusion imaging, provides incremental information over the perfusion data, and has shown potentials for myocardial viability assessment and sequential follow-up after therapy. After reading this article, the readers will understand (a) the general principles of GSPECT and quantitation, (b) the methods of the image acquisition and analysis, (c) validation of GSPECT with other cardiac imaging modalities, and (d) application of the GSPECT-derived functional parameters in the clinical practice.

Key Words: cardiology; electrocardiographic gating; gated myocardial perfusion SPECT; left ventricular function

J Nucl Med Technol 2004; 32:179–187

Evaluation of the left ventricular (LV) function is important in clinical cardiology. Quantifying the degree and extent of the LV functional abnormalities permits a systematic assessment of the disease process on the myocardial performance, provides an objective basis for the risk stratification and therapeutic strategy, and allows for the sequential follow-up of the therapeutic response. Since its introduction in the late 1980s, electrocardiographically (ECG) gated myocardial perfusion SPECT (GSPECT) has been increasingly used for the assessment of the LV function in the clinical setting. ECG gating of a standard myocardial perfusion SPECT acquisition allows for the quantitative or semiquantitative assessment of the LV function simultaneously with the evaluation of the LV perfusion (*1*). LV functional indices, obtained by GSPECT, aid in the diagnosis (*2–4*), assessment of the risk and prognosis (*5–9*), determination of the myocardial viability (*10–12*), and evaluation of the functional recovery after the revascularization procedure (*13,14*) in patients with known or suspected coronary artery disease (CAD). GSPECT often provides incremental information over the perfusion data (*3,4,7*). This article focuses on the assessment of the LV function using GSPECT. General principles, methods of the image acquisition and analysis, and clinical applications of GSPECT are discussed.

Three γ-camera imaging techniques are available to measure the ventricular function: first-pass radionuclide angiography (FPRNA), equilibrium gated radionuclide angiography (ERNA), and GSPECT. During FPRNA, a dynamic bolus of radioactivity is imaged as it quickly transits through different chambers of the heart and lungs. It is a preferred technique for the assessment of peak-exercise ventricular function, measurement of the right ventricular (RV) function, and quantification of the cardiac shunt (*15*). Both acquisitions of ERNA and GSPECT are synchronized with the subject's ECG, which identifies the temporal phases of the cardiac cycle. But there are fundamental differences between these 2 procedures. During an ERNA study, a blood-pool agent such as ^{99m}Tc-labeled erythrocytes is injected. Images are acquired over many hundreds of heartbeats after the administered radioactivity has equilibrated in the vascular space. Ventricular cavity counts are used to generate a time–activity curve, from which functional parameters are derived. During a GSPECT study, a perfusion tracer is injected. The tracer is taken up by the LV myocardium. Definition of the LV myocardium and LV cavity is achieved by delineating the epicardial and endocardial edges on the perfusion image. LV global and re-

For correspondence or reprints contact: Asit K. Paul, MBBS, PhD, Department of Nuclear Medicine, State University of New York, University at Buffalo, 105, Parker Hall, 3435 Main St., Buffalo, NY 14214.
E-mail: asitpaul@buffalo.edu

gional contractile function is quantitated based on the changes in the LV volume, excursion of the endocardium, and brightening of the myocardium from the end-diastolic image to the end-systolic image, as identified by the ECG. Because RV myocardium is not adequately visualized on the perfusion images, GSPECT is not suitable for accurate RV function measurement.

ERNA is independent of the geometric assumption and has been used as a standard technique for ventricular function measurements for many years (*16*). Despite its accuracy and reproducibility, there has been a decline in this procedure in recent years, mainly because of the widespread availability of echocardiography in clinical settings. In contrast, GSPECT continues to grow (*17*). A consistent growth has been observed over the last decade. Several factors contributed to its popularity. First, GSPECT is a simple method to evaluate the LV perfusion and function within a single study. Functional status of a hypoperfused or normally perfused area has great clinical relevance. This advantage has made it a method of choice in patients with CAD. Second, favorable kinetics of the ^{99m}Tc-labeled perfusion tracers—in particular, sestamibi and tetrofosmin—allow ECG gating with flexible acquisition protocols. Third, current advances in multidetector γ-cameras and computers have shortened the acquisition and processing time significantly. Moreover, automation of the image processing and quantification has made this technique simple, practical, and user friendly in clinical settings (*18–22*). This has significantly improved the reproducibility of the measurements (*23–25*). Fourth, GSPECT measurements have been extensively validated against many other standard cardiac imaging modalities (*26–41*).

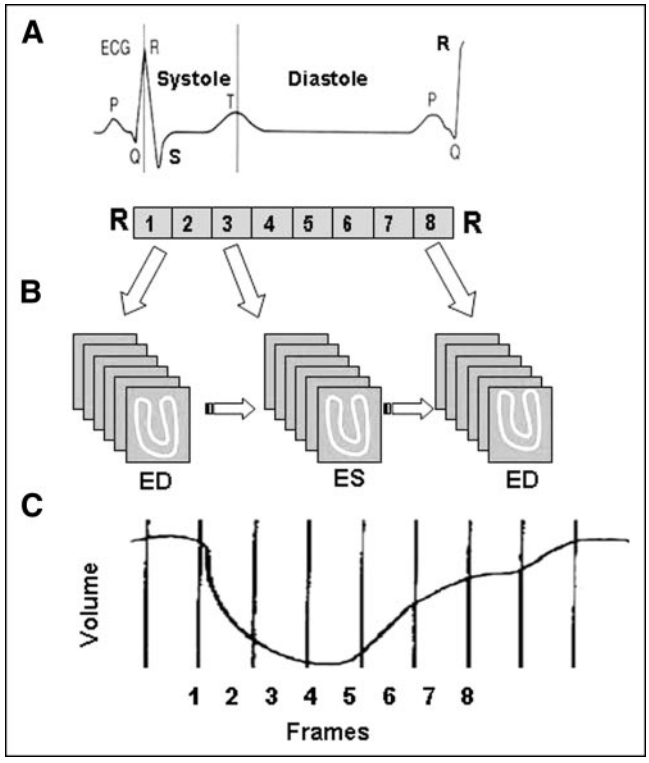

FIGURE 1. Principle of ECG-gated acquisition. R–R interval on ECG, representing 1 cardiac cycle, is typically divided into 8 frames of equal duration (A). Image data from each frame are acquired over multiple cardiac cycles and stored separately in specific locations ("bin") of computer memory (B). When all data in a bin are added together, image represents a specific phase of cardiac cycle. Typically, a volume curve is obtained, which represents endocardial volume for each of 8 frames (C). ED = end-diastole; ES = end-systole.

GENERAL PRINCIPLES

Gating

The fundamental principle of ECG gating is illustrated in Figure 1. During a SPECT acquisition, a γ-camera records the photons at multiple projection angles around the subject along a 180° or 360° arc. At each of the projection angles, one static image is acquired during an ungated image acquisition, whereas several dynamic images spanning the length of the cardiac cycle are acquired at equal intervals during an ECG-gated acquisition. Acquisition starts with the R wave on the ECG, which corresponds to the end-diastole. One cardiac cycle, represented by the R–R interval, is divided into multiple frames of equal duration. Image data for each of the frames are acquired repeatedly over many cardiac cycles and stored separately in the computer. During processing, all data of a particular frame are added together to construct a specific phase of the cardiac cycle. When all temporal frames are summed together, this is equivalent to a standard set of ungated perfusion images.

Framing

In routine practice, acquisition of 8 frames per cardiac cycle is considered satisfactory. This allows the acquisition to be completed within a reasonable time, while sufficient counts are collected for optimal image quality. When a greater number of frames is acquired, better temporal resolution is achieved. But with an increased number of frames, each frame is of shorter duration and the acquisition has to be prolonged to collect adequate counts. The LV ejection fraction (LVEF) measured from the 8-frame acquisition has been reported to be 3 units lower than that of the 16-frame acquisition, but the relationship is fairly uniform (*18*). With the availability of multidetector cameras and faster computers, a greater number of frames can be acquired without a significant increase in the acquisition or processing time.

Heartbeat Variation and Tolerance

Adequate count density in a frame is a prerequisite for a quality GSPECT study. Too few counts in a frame may cause a "flashing" artifact, which appears as a streak defect on the reconstructed images (*1*). To achieve adequate count density in each frame, gated data are acquired over many cardiac cycles. But all cardiac cycles may not be of equal duration. The variation in the length of the cardiac cycle may cause mixing of counts from adjacent frames (temporal blurring) and compromise the quality of the study. Most commercial systems now offer beat-rejection software to acquire data with a stable R–R interval. The computer

determines the length of the cardiac cycle based on the average of multiple R–R intervals before the acquisition. A range of acceptable beats ("acceptance window") is specified. This is known as "tolerance" and is expressed as the percentage of the mean R–R interval. For example, a tolerance of 20% allows acquiring data from cardiac cycles having a duration within ±10% of the mean R–R interval. The duration of one cardiac cycle in a subject with an average heart rate of 72 beats per minute is 0.8 s. Therefore, with a 20% tolerance, all beats having duration of 0.72–0.88 s will be acquired and cardiac cycles outside this range will be rejected. When the window is narrow, arrhythmic beats are avoided but the acquisition may be prolonged significantly. If the window is too wide, arrhythmic beats may be included.

Quantitation

The approaches of the quantitation vary according to the nature of the quantitative algorithm used (*18–22*). Only general principles are outlined here. Quantification starts with the detection of the LV endocardial and epicardial boundaries. Most algorithms first estimate the location of the midmyocardium, which corresponds to the maximal myocardial count. From the midmyocardial points, endocardial and epicardial boundaries can be extracted either by using a fixed number of SDs of gaussian fitting to the myocardial count profile (*18,19*) or using a predefined count threshold based on the phantom data (*20*). Once the definitions of the endocardial and epicardial edges are achieved, the area bounded by the endocardial surface and the mitral valve represents the LV cavity, and the area bounded by the endocardium, epicardium, and mitral valve plane represents the LV myocardium. LV volume is calculated by multiplying the number of pixels within the LV cavity with the size of a pixel. LV volume can be generated for each of the frames in the cardiac cycle. The largest volume and the smallest volume represent the end-diastolic volume (EDV) and the end-systolic volume (ESV), respectively. LVEF is derived from the volumes using the formula (EDV − ESV)/EDV × 100. Once the endocardial edge is detected, regional endocardial wall motion (RWM) can be quantitated by computing the distance of a given point on the endocardial surface between end-diastole and end-systole. Measurement of the systolic wall thickening (SWT) is based on the principle of the partial-volume effect (*42*). According to this principle, when the size of the object is less than twice the resolution of the γ-camera, a change in the size of an object (such as myocardial wall) results in a change in its apparent concentration of counts. Because current γ-camera systems have a resolution on the order of 1 cm, this relationship is valid for the majority of cases in which the myocardial thickness ranged from 0.5 to 2.0 cm. The count density is therefore linearly related to the increase in wall thickness (brightness) during myocardial contraction (*43*). However, absolute thickness cannot be measured. The relative or percentage changes in thickness can be assessed from the changes in the count density from the end-diastole frame to the end-systole frame.

ACQUISITION AND ANALYSIS

Radiotracers

^{201}Tl, ^{99m}Tc-sestamibi, and ^{99m}Tc-tetrofosmin are 3 routinely used myocardial perfusion imaging tracers. Due to the shorter half-life, a higher dose of ^{99m}Tc (half-life, 6 h) can be administered to a patient than that of ^{201}Tl (half-life, 73 h) without associated increase in the radiation burden. A higher dose results in better count statistics in the images and is associated with lower statistical error and better image quality. Therefore, from a practical standpoint, ^{99m}Tc-sestamibi or ^{99m}Tc-tetrofosmin is the preferred agent for a GSPECT study. With the availability of multidetector γ-cameras, which allow a better counting efficiency than single-detector cameras, gated acquisition with ^{201}Tl is now feasible (*44*).

Protocols

Standard myocardial perfusion SPECT can be gated at rest or after exercise–stress, as long as the count rate is adequate. A same-day or separate-day protocol can be used. When one acquisition is gated, the higher dose study is preferred for the gating (Fig. 2). One common approach is to gate

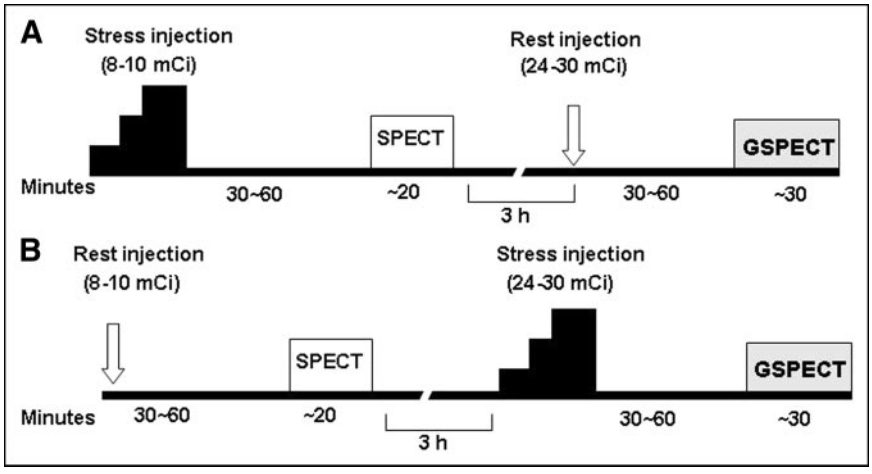

FIGURE 2. Same-day GSPECT protocols with ^{99m}Tc-sestamibi or ^{99m}Tc-tetrofosmin. Myocardial perfusion imaging can be gated either at rest or after exercise–stress in stress–rest (A) or rest–stress (B) sequence.

the stress study either as a part of a low-dose rest/high-dose stress ^{99m}Tc or a rest ^{201}Tl/stress ^{99m}Tc (dual isotope) sequence. With ^{99m}Tc tracers, imaging is performed 30–60 min after the injection to allow clearance of the adjacent extracardiac activities. Because sestamibi or tetrofosmin shows minimal redistribution, the perfusion pattern reflects the myocardial distribution of the tracer at the time of injection (peak stress), whereas function represents the LV function at the time of acquisition. In healthy subjects or patients with previous myocardial infarction, poststress gated images thus represent stress perfusion and rest function. However, stress-induced LV dysfunction in patients with severe ischemia may be continued for a prolonged period, resulting in a reduced function during the poststress acquisition compared with the resting basal function (*23,45–47*). Many centers now prefer to gate both the rest and the stress acquisitions to evaluate this phenomenon. A standard GSPECT acquisition is generally completed within 20–30 min. Although a GSPECT protocol as short as 7 min has been described in the literature (*48*), assessment of the stress ventricular function is routinely not feasible with a routine GSPECT study. Protocols have also been developed for viability assessment. In these protocols, the tracer is injected at rest and gated acquisition is performed during infusion of an inotropic agent (low-dose dobutamine) (*49*).

Patients, Acquisition, and Reconstruction

Patients with sinus rhythm are ideal candidates for GSPECT studies. Mild tachycardia or bradycardia is acceptable to the extent that regularity of the heartbeat is not affected. GSPECT should not be performed in patients with severe arrhythmia, such as atrial fibrillation, frequent premature ectopic beats, and heart block. Image acquisition is similar to a standard perfusion SPECT acquisition except a 3-lead ECG provides the mechanism for gating. When the R wave on the ECG is detected, the gating device interfaced to the acquisition computer sends a signal to start the acquisition. Standard acquisition parameters are shown in Table 1. After the acquisition is completed, identical raw image data are used for the perfusion and function analysis. For perfusion analysis, the frames are summed together, reconstructed, and displayed in standard vertical long-axis, horizontal long-axis, and short-axis slices. For functional analysis, raw data are reconstructed frame by frame. Because of the relatively poor counts, gated projection data require more smoothing than ungated or summed data during the reconstruction. Before reconstruction, it is important to check the raw projection data for potential sources of errors and artifacts. Any error during image acquisition (instruments, patient motion, soft-tissue attenuation artifacts, severe arrhythmia) or reconstruction (inappropriate filter and cutoff) is likely to be propagated and will compromise the accuracy of the measurements.

TABLE 1
Acquisition Parameters for GSPECT with ^{99m}Tc-Perfusion Tracers

Parameter	Characteristic
γ-Camera	Dual or triple detector
Collimator	Low energy, high resolution
Orbit	180° (dual detector) or 360° (triple detector)
Projections	32~64
Acquisition time/projection	>25 s
Matrix	64 × 64
Framing	8~16/R–R interval
Beat acceptance	±20%
Total acquisition time	~20–30 min

Measurement and Analysis

LV volumes and LVEF can be obtained easily by applying one commercially available software to the reconstructed gated dataset. Software packages developed at Cedars-Sinai Medical Center (QGS) (*18,19*), University of Michigan (4D-MSPECT), and Emory University (Emory Cardiac Toolbox) (*21*) are widely available. Direct comparison among these software packages showed excellent correlations in LV volumes and LVEF measurements (*50–52*). LV regional function is more commonly evaluated visually on a cine-loop display. RWM is assessed by evaluating the endocardial border excursion, and SWT is assessed by evaluating the changes in brightness (count intensity) from the end-diastolic to the end-systolic frame (Fig. 3). Some programs (e.g., QGS) offer automatic quantitative indices of RWM (in mm) and SWT (% diastolic thickness), which are displayed on a segmental, circumferential model of the LV with each segment representing a particular territory of the LV (*19*). In addition, several studies have recently reported the measurement of the LV diastolic indices (*53*) and LV mass (*54,55*) from GSPECT. However, clinical utilization of these indices is still in the preliminary stage (*56,57*).

All functional indices should be interpreted in reference to the age- and sex-specific normal database. Because the approaches of quantification vary, definition of the normal limits and criteria for abnormalities for a specific quantitative program are essential for optimal interpretation. Normal ranges of the LVEF and regional functional parameters for different programs have been reported (*58–60*). It is important to realize that there are considerable variations and heterogeneity in RWM and SWT even in healthy subjects (*58*). Definition of the normal limits for each LV region is therefore desirable. For visual analysis, the reader should be familiar with the pattern of the normal LV contraction in different segments of the LV. The accuracy of GSPECT largely depends on the proper delineation of the endocardial contour. In the presence of a severe perfusion defect, large aneurysmal dilatation, or significant structural distortion of the LV, the edge detection is often inaccurate (*61*). Accuracy is also limited in patients with a smaller heart (women and pediatric population). There is an apparent shrinkage in the LV cavity due to the partial-volume effect and a relatively low resolution of the images. The ESV is underestimated more than the EDV, resulting in an

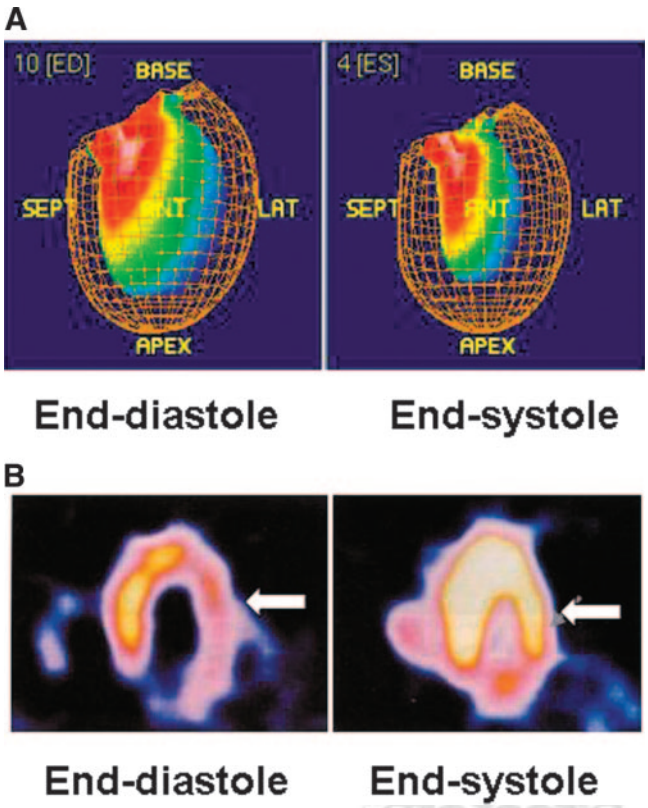

FIGURE 3. Assessment of LV regional function by GSPECT. RWM is assessed by inward excursion of endocardial wall (A) and SWT is assessed by myocardial brightening (arrow) from end-diastole to end-systole (B). ED = end-diastole; ES = end-systole; SEPT = septal; ANT = anterior; LAT = lateral.

overestimation of the LVEF (*62*). Zooming during the acquisition or reconstruction may reduce this error.

VALIDATION

The automatic, operatorless quantitative programs have almost eliminated subjectivity and demonstrated excellent inter- and intraobserver reproducibility (*31*). However, repeatability, which is reproducibility of the measurements obtained from 2 consecutive acquisitions on the same subject, can be affected by several factors such as image acquisition, data processing, quantification, as well as physiologic variation of the subject being studied. Some of the published studies on the repeatability using a popular quantitative program are summarized in Table 2 (*23–25*).

LV volumes and LVEF measurements obtained by GSPECT have been extensively validated against other imaging modalities including cardiac MRI (*26–29*), contrast ventriculography (*30,31*), echocardiography (*32,33*), and tomographic and planar ERNA (*34,35*) (Table 3). An example of the GSPECT LVEF in comparison with the contrast left ventriculography is shown in Figure 4. MRI is currently considered as the gold standard for ventricular volumes and function measurements (*63*). Two meta-analysis studies have recently been published comparing LV volumes and LVEF measurements between GSPECT and MRI (*36,37*). One study included 164 subjects from 9 studies (*36*). GSPECT tends to overestimate EDV and ESV compared with MRI at higher volumes and underestimate LVEF when LVEF is very low. Although the individual values vary, there are excellent overall correlations between these 2 modalities: EDV, $r = 0.89$; ESV, $r = 0.92$; and LVEF, $r = 0.87$. The visual estimates of RWM and SWT agree well with other modalities, including MRI and echocardiography (*38–41*) (Table 4). To date, quantitative RWM and SWT data have been compared only with expert visual analysis (*19,58*). Their accuracy in comparison with other independent modalities such as MRI is currently unknown.

CLINICAL APPLICATIONS

A number of studies have demonstrated the clinical usefulness of GSPECT (*64–66*). Because patients with known or suspected CAD constitute the majority of those referred for perfusion imaging, most of the studies have been performed on CAD patients. The value of GSPECT in the differentiation of attenuation artifacts (*2*), improved detection of 3-vessel CAD (*3*), diagnosis of CAD in women (*4*), and assessment of ischemic severity (*8,67*) is well documented. The role in risk stratification (*5,6*), prognostication

TABLE 2
Repeatability of Gated SPECT Measurements

Reference					
Year	Author	Parameter	No. of patients	Measurement	Agreement
1997	Johnson et al. (*23*)	LVEF	15	Consecutive days	$r = 0.98$, SD = 2.6%
1998	Berman et al. (*24*)	LVEF	180	Prone	$r = 0.93$, SD = 3.2%
		EDV	180	Supine	$r = 0.97$, SD = 2.6 mL
		ESV	180	Same-day consecutive scans	$r = 0.98$, SD = 4.8 mL
2001	Paeng et al. (*25*)	RWM	31	Same-day consecutive scans	$r = 0.95$ (quantitative); 79%*, $\kappa = 0.81$ (visual)
		SWT	31	Same-day consecutive scans	$r = 0.88$ (quantitative); 71%*, $\kappa = 0.71$ (visual)

*Exact segmental agreement.

κ = Cohen's κ.

Measurements were performed using QGS software (*18,19*).

TABLE 3
Validation of LV Volumes and EF Measurements Obtained by GSPECT

Reference		Study patients	No. of patients	Modality of comparison	*r* with GSPECT measurements		
Year	Author				EDV	ESV	LVEF
1999	Vaduganathan et al. (*26*)	Recent MI	25	MRI	0.81	0.92	0.93
1999	Tadamura et al. (*27*)	CAD	20	MRI	0.92	0.97	0.94
2000	Bavelaar-Croon et al. (*28*)	CAD	21	MRI	0.94	0.95	0.85
2000	Bax et al. (*29*)	CAD with LV dysfunction	25	MRI	0.84	0.87	0.90
1998	Nichols et al. (*30*)	CAD	58	LVG	0.87	0.91	0.86
1999	Yoshioka et al. (*31*)	Mixed	21	LVG	0.73	0.83	0.87
1999	Cwajg et al. (*32*)	Mixed	109	Echo	0.87	0.86	0.72
2001	Vourvouri et al. (*33*)	CAD with LV dysfunction	32	Echo	0.94	0.96	0.83
2000	Paul et al. (*34*)	Mixed	15	ERNA (tomographic)	0.99	0.99	0.97
2000	Chua et al. (*35*)	CAD with large defect	62	ERNA (planar)	0.88	0.95	0.94

MI = myocardial infarction; LVG = contrast left ventriculography; Echo = echocardiography.

(*7,9*), viability assessment (*10–12*), and follow-up after revascularization (*13,14*) is still evolving.

Diagnosis

The diagnostic role of myocardial perfusion SPECT in patients with CAD is well recognized. Gating provides additional information that cannot be obtained by perfusion imaging alone. For example, a normal perfusion study in a patient undergoing screening generally carries an excellent prognostic value (*68*). An abnormally low LVEF in this patient may alert the physician to look for other comorbidities, whereas a normal function and perfusion obviate the need for further invasive cardiac investigations. In patients with 3-vessel coronary disease, perfusion abnormalities may not always be evident in all vascular territories because of the globally reduced perfusion. In a recent study that included 143 patients with angiographically proven 3-vessel disease, combined perfusion–function assessment by GSPECT has been shown to yield significantly more abnormal segments in comparison with perfusion alone (*3*). Combined perfusion–function analysis can also differentiate ischemic from nonischemic, dilated cardiomyopathy (*69*). Although both the perfusion and the LV function are abnormal in patients with ischemic cardiomyopathy, LV dysfunction is present without any significant perfusion abnormalities in patients with nonischemic cardiomyopathy.

One well-recognized application of GSPECT is to classify a fixed perfusion defect as a soft-tissue attenuation artifact or an infarct (*2*). The common sites of attenuation are left breast (anterior wall), subcutaneous fat (lateral wall), and left hemidiaphragm (inferior wall). Attenuation artifacts increase the false-positive interpretation of the perfusion scans in obese patients and in female patients. Because an artifactual defect would show normal contraction (wall motion or thickening) on a gated image, artifacts can be differentiated from a true infarct (Fig. 5). This has great clinical value in women, because a stress ECG, like perfusion imaging, also has a high false-positive rate in this patient population (*4*). Gating also increases the reader's confidence in interpretation of the perfusion scan, as evidenced by a decrease in the number of perfusion scans reported as equivocal or borderline to normal or abnormal (*70*).

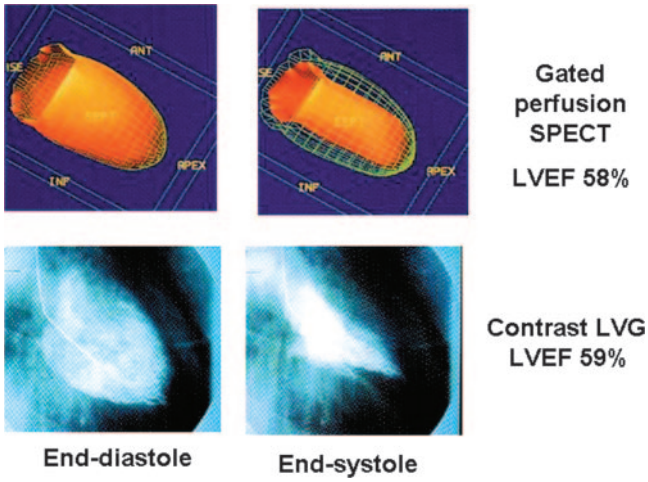

FIGURE 4. Comparison of LVEF between GSPECT and contrast left ventriculography (LVG) in a patient. ISE = base; ANT = anterior; SEPT = septal; INF = inferior.

Assessment of Severity

Exercise-induced angina produces defects in stress perfusion images and is associated with LV contractile dysfunction. In most patients, these abnormalities quickly return to baseline (reversible) after cessation of the exercise. But more than one third of the ischemic patients show persistent dysfunction as late as 1 h after the exercise (*45–47*). Persistent LV dysfunction on poststress GSPECT predicts a high-grade coronary stenosis (*67*) and can be used as a noninvasive marker of the disease severity (*8*). The magnitude of the poststress regional or global dysfunction correlates with the severity of the ischemia (*46,47*). Furthermore, it has been shown that a poststress wall motion abnormality (stress-induced stunning) is more sensitive than a resting and stress wall motion abnormality and is highly specific for a severe angiographic stenosis (*67*).

TABLE 4
Validation of LV Regional Function Obtained by GSPECT

Reference		Patients	No. of patients	No. of segments	GSPECT evaluation	Modality of comparison	Exact agreement, κ value	
Year	Author						RWM	SWT
1997	Gunning et al. (*38*)	Mixed	28	252	Visual, SQ	MRI	78%, 0.66	78%, 0.62
1999	Tadamura et al. (*27*)	CAD	20	180	Visual, SQ	MRI	84%, 0.73	87%, 0.76
1999	Tadamura et al. (*39*)	After CABG	16	128	Visual, SQ	MRI	NA	76%, 0.62
2001	Wahba et al. (*40*)	CAD	21	273	Visual, SQ	MRI	84%, 0.72	86%, 0.77
1994	Chua et al. (*41*)	CAD	40	640	Visual, SQ	Echo	91%, 0.68	90%, 0.62
1997	Germano et al. (*19*)	Mixed	79	1,580	Quantitative	Visual, SQ GSPECT	73%, 0.43	75%, 0.41
2000	Sharir et al. (*58*)	Mixed	100	2,000	Quantitative	Visual, SQ GSPECT	80%, 0.71	86%, 0.68

κ = Cohen's κ; SQ = semiquantitative; CABG = coronary artery bypass graft; NA = not available; Echo = echocardiography.

Risk Stratification and Prognosis

LV functional status is well recognized as a predictor of future cardiac events after myocardial infarction. GSPECT can be used to estimate the residual function after myocardial infarction (*71*). Patients can be risk stratified on the basis of the LVEF and LV volumes. Poststress LVEF and ESV obtained from GSPECT provide incremental information over the perfusion and prescan clinical data in the prediction of cardiac death as well as the combined endpoint of cardiac death or myocardial infarction. Sharir et al. showed that patients with an LVEF $\geq 45\%$ or an ESV ≤ 70 mL had a lower mortality rate, despite severe perfusion abnormalities, whereas patients with an LVEF $< 45\%$ or an ESV > 70 mL had a higher mortality rate, even with mild-to-moderate perfusion abnormalities (*7*). When cardiac death and nonfatal myocardial infarction are considered as separate endpoints, poststress LVEF is the best predictor of cardiac death, whereas the amount of ischemia is the best predictor of nonfatal infarction (*5*). GSPECT is also useful in preoperative risk assessment of patients undergoing major noncardiac surgery and may predict perioperative cardiac events (*6*).

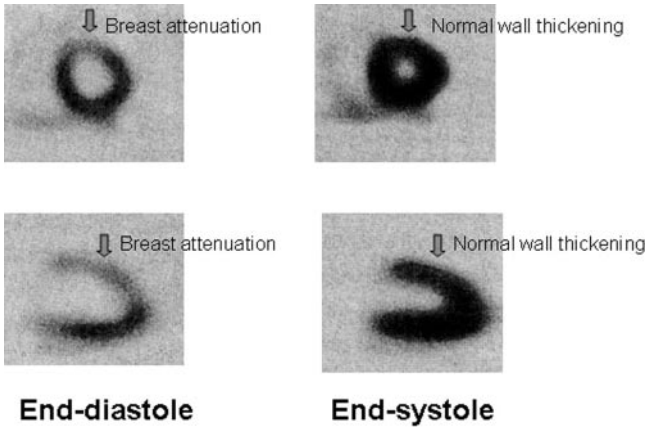

FIGURE 5. GSPECT shows preserved SWT of anterior wall of LV, suggesting presence of attenuation artifact rather than true infarct.

Myocardial Viability

Restoration of the blood flow by surgical revascularization is an important modality of treatment in patients with chronic CAD and LV dysfunction. Dysfunctional but viable myocardium is potentially reversible, and patients often benefit from surgery in terms of quality of life and survival. On the other hand, surgery in a true infarct or necrotic myocardium is unnecessary and is associated with significant operative morbidity and mortality. Thus, differentiation of the viable myocardium from the nonviable myocardium before surgical intervention is crucial. Perfusion–metabolism mismatch—that is, preserved metabolism (as shown by PET) in an area of decreased perfusion—is considered as the gold standard for myocardial viability assessment. Recent studies have expanded the potential application of GSPECT in the assessment of viability (*10–12*). A high predictive value for the functional recovery after surgical revascularization has been documented (*11,12*). GSPECT relies on demonstration of the regional contractile function in a hypoperfused area as an indication of the viability. Whereas preservation of function is clearly proof of viability, absence of function does not necessarily indicate absence of viability. This is because chronically ischemic myocardium, so-called hibernating myocardium, may have greatly reduced or absent systolic function. This limitation can be overcome by using inotopic stimulation of the heart. Regional contractile function may be abnormal at rest, but improved contractility after infusion of an inotropic agent (e.g., dobutamine at low dose) may differentiate the viable myocardium (positive contractile reserve) from the nonviable, scarred myocardium (negative contractile reserve) (*49*).

Follow-Up After Revascularization

The excellent reproducibility and repeatability of GSPECT are particularly suited to assess the functional changes after coronary revascularization. LV functional status can be compared before and after the revascularization procedure. Functional improvement after coronary artery bypass grafting (CABG) or percutaneous angioplasty is evident by an increase in the LVEF, a decrease in the ESV, and an improvement in the regional contractile function

(*13,14*). SWT analysis has an advantage over RWM analysis in the post-CABG setting. Post-CABG patients generally show abnormal wall motion of the septum, despite no significant myocardial damage. It is thought to be artifactual and a result of exaggerated systolic anteromedial cardiac translation after surgery. SWT is preserved in that region and is considered a better marker of regional contractile function than RWM in these patients (*13*). However, evaluation too early may not show adequate functional recovery, despite restoration of the perfusion due to stunning (*72*).

CONCLUSION

GSPECT is a simple way of obtaining the LV function along with the perfusion within a single study. The functional parameters are objective, reproducible, and extensively validated. The continued and substantial growth of GSPECT procedures in recent years reflects its clinical utility. The current trend clearly indicates that GSPECT will continue to be the most commonly performed nuclear cardiology procedure in coming years. However, proper patient selection, adequate quality control, identification of the technical limitations, and application in appropriate clinical situations are important prerequisites for the optimal utilization of this modality.

ACKNOWLEDGMENT

The authors thank Elpida S. Crawford, director of the Nuclear Medicine Technology Program at the State University of New York at Buffalo, for her critical review of the manuscript.

REFERENCES

1. Cullom SJ, Case JA, Bateman MD. Electrocardiographically gated myocardial perfusion SPECT: technical principles and quality control considerations. *J Nucl Cardiol.* 1998;5:418–425.
2. DePuey EG, Rozanski A. Using gated technetium-99m-sestamibi SPECT to characterize fixed myocardial defects as infarct or artifact. *J Nucl Med.* 1995;36:952–955.
3. Lima RS, Watson DD, Goode AR, et al. Incremental value of combined perfusion and function over perfusion alone by gated SPECT myocardial perfusion imaging for detection of severe three-vessel coronary artery disease. *J Am Coll Cardiol.* 2003;42:64–70.
4. Taillefer R, DePuey EG, Udelson JE, Beller GA, Latour Y, Reeves F. Comparative diagnostic accuracy of Tl-201 and Tc-99m sestamibi SPECT imaging (perfusion and ECG-gated SPECT) in detecting coronary artery disease in women. *J Am Coll Cardiol.* 1997;29:69–77.
5. Sharir T, Germano G, Kang X, et al. Prediction of myocardial infarction versus cardiac death by gated myocardial perfusion SPECT: risk stratification by the amount of stress-induced ischemia and the poststress ejection fraction. *J Nucl Med.* 2001;42:831–837.
6. Hashimoto J, Suzuki T, Nakahara T, Kosuda S, Kubo A. Preoperative risk stratification using stress myocardial perfusion scintigraphy with electrocardiographic gating. *J Nucl Med.* 2003;44:385–390.
7. Sharir T, Germano G, Kavanagh PB, et al. Incremental prognostic value of poststress left ventricular ejection fraction and volume by gated myocardial perfusion single photon emission computed tomography. *Circulation.* 1999; 100:1035–1042.
8. Sharir T, Bacher-Stier C, Dhar S, et al. Identification of severe and extensive coronary artery disease by postexercise regional wall motion abnormalities in Tc-99m sestamibi gated single-photon emission computed tomography. *Am J Cardiol.* 2000;86:1171–1175.
9. Kang WJ, Lee DS, Paeng JC, Kim KB, Chung JK, Lee MC. Prognostic value of rest ^{201}Tl-dipyridamole/stress ^{99m}Tc-sestamibi gated SPECT for predicting patient-based clinical outcomes after bypass surgery in patients with ischemic left ventricular dysfunction. *J Nucl Med.* 2003;44:1735–1740.
10. Maruyama A, Hasegawa S, Paul AK, et al. Myocardial viability assessment with gated SPECT Tc-99m tetrofosmin % wall thickening: comparison with FDG PET. *Ann Nucl Med.* 2002;16:25–32.
11. Stollfuss JC, Haas F, Matsunari I, et al. ^{99m}Tc-Tetrofosmin SPECT for prediction of functional recovery defined by MRI in patients with severe left ventricular dysfunction: additional value of gated SPECT. *J Nucl Med.* 1999;40:1824–1831.
12. Levine MG, McGill CC, Ahlberg AW, et al. Functional assessment with electrocardiographic gated single-photon emission tomography improves the ability of technetium-99m sestamibi myocardial perfusion imaging to predict myocardial viability in patients undergoing revascularization. *Am J Cardiol.* 1999;83:1–5.
13. Taki J, Higuchi T, Nakajima K, et al. Electrocardiographic gated ^{99m}Tc-MIBI SPECT for functional assessment of patients after coronary artery bypass surgery: comparison of wall thickening and wall motion analysis. *J Nucl Med.* 2002;43:589–595.
14. Hida S, Chikamori T, Usui Y, Yanagisawa H, Morishima T, Yamashina A. Effect of percutaneous coronary angioplasty on myocardial perfusion, function, and wall thickness as assessed by quantitative gated single-photon emission computed tomography. *Am J Cardiol.* 2003;91:591–594.
15. Nichols K, DePuey EG, Rozanski A. First-pass radionuclide angiocardiography with single-crystal gamma cameras. *J Nucl Cardiol.* 1997;4:61–73.
16. Adam WE, Clausen M, Hellwig D, Henze E, Bitter F. Radionuclide ventriculography (equilibrium gated blood pool scanning): its present clinical position and recent developments. *Eur J Nucl Med.* 1988;13:637–647.
17. Bonow RO. Gated myocardial perfusion imaging for measuring left ventricular function [editorial]. *J Am Coll Cardiol.* 1997;30:1649–1650.
18. Germano G, Kiat H, Kavanagh PB, et al. Automatic quantification of ejection fraction from gated myocardial perfusion SPECT. *J Nucl Med.* 1995;36:2138–2147.
19. Germano G, Erel J, Lewin H, Kavanagh PB, Berman DS. Automatic quantitation of regional myocardial wall motion and thickening from gated technetium-99m sestamibi myocardial perfusion single-photon emission computed tomography. *J Am Coll Cardiol.* 1997;30:1360–1367.
20. DePuey EG, Nichols K, Dobrinsky C. Left ventricular ejection fraction assessed from technetium-99m-sestamibi SPECT. *J Nucl Med.* 1993;34: 1871–1876.
21. Faber TL, Cooke CD, Folks RD, et al. Left ventricular function and perfusion from gated perfusion images: an integrated method. *J Nucl Med.* 1999;40:650–659.
22. Everaert H, Franken PR, Flamen P, et al. Left ventricular ejection fraction from gated SPECT myocardial perfusion studies: a method based on the radial distribution of count rate density across the myocardial wall. *Eur J Nucl Med.* 1996;23:1628–1633.
23. Johnson LL, Verdesca SA, Aude WY, et al. Postischemic stunning can affect left ventricular ejection fraction and regional wall motion on poststress gated sestamibi tomograms. *J Am Coll Cardiol.* 1997;30:1641–1648.
24. Berman D, Germano G, Lewin H, et al. Comparison of post-stress ejection fraction and relative left ventricular volumes by automatic analysis of gated myocardial perfusion single-photon emission computed tomography acquired in the supine and prone positions. *J Nucl Cardiol.* 1998;5:40–47.
25. Paeng JC, Lee DS, Cheon GJ, Lee MM, Chung JK, Lee MC. Reproducibility of an automatic quantitation of regional myocardial wall motion and systolic thickening on gated ^{99m}Tc-sestamibi myocardial SPECT. *J Nucl Med.* 2001;42:695–700.
26. Vaduganathan P, He ZX, Vick GW 3rd, Mahmarian JJ, Verani MS. Evaluation of left ventricular wall motion, volumes, and ejection fraction by gated myocardial tomography with technetium 99m-labeled tetrofosmin: a comparison with cine magnetic resonance imaging. *J Nucl Cardiol.* 1999; 6:3–10.
27. Tadamura E, Kudoh T, Motooka M, et al. Assessment of regional and global left ventricular function by reinjection T1–201 and rest Tc-99m sestamibi ECG-gated SPECT: comparison with three-dimensional magnetic resonance imaging. *J Am Coll Cardiol.* 1999;33:991–997.
28. Bavelaar-Croon CD, Kayser HW, van der Wall EE, et al. Left ventricular function: correlation of quantitative gated SPECT and MR imaging over a wide range of values. *Radiology.* 2000;217:572–575.
29. Bax JJ, Lamb H, Dibbets P, et al. Comparison of gated single-photon emission computed tomography with magnetic resonance imaging for evaluation of left ventricular function in ischemic cardiomyopathy. *Am J Cardiol.* 2000;86:1299–1305.
30. Nichols K, Tamis J, DePuey EG, Mieres J, Malhotra S, Rozanski A.

Relationship of gated SPECT ventricular function parameters to angiographic measurements. *J Nucl Cardiol*. 1998;5:295–303.
31. Yoshioka J, Hasegawa S, Yamaguchi H, et al. Left ventricular volumes and ejection fraction calculated from quantitative electrocardiographic-gated ^{99m}Tc-tetrofosmin myocardial SPECT. *J Nucl Med.* 1999;40:1693–1698.
32. Cwajg E, Cwajg J, He ZX, et al. Gated myocardial perfusion tomography for the assessment of left ventricular function and volumes: comparison with echocardiography. *J Nucl Med.* 1999;40:1857–1865.
33. Vourvouri EC, Poldermans D, Bax JJ, et al. Evaluation of left ventricular function and volumes in patients with ischaemic cardiomyopathy: gated single-photon emission computed tomography versus two-dimensional echocardiography. *Eur J Nucl Med.* 2001;28:1610–1615.
34. Paul AK, Hasegawa S, Yoshioka J, Yamaguchi H, Tsujimura E, Nishimura T. Assessment of left ventricular function by gated myocardial perfusion and gated blood-pool SPECT: can we use the same reference database? *Ann Nucl Med.* 2000;14:75–80.
35. Chua T, Yin LC, Thiang TH, Choo TB, Ping DZ, Leng LY. Accuracy of the automated assessment of left ventricular function with gated perfusion SPECT in the presence of perfusion defects and left ventricular dysfunction: correlation with equilibrium radionuclide ventriculography and echocardiography. *J Nucl Cardiol.* 2000;7:301–311.
36. Ioannidis JP, Trikalinos TA, Danias PG. Electrocardiogram-gated single-photon emission computed tomography versus cardiac magnetic resonance imaging for the assessment of left ventricular volumes and ejection fraction: a meta-analysis. *J Am Coll Cardiol.* 2002;39:2059–2068.
37. Kondo C, Fukushima K, Kusakabe K. Measurement of left ventricular volumes and ejection fraction by quantitative gated SPECT, contrast ventriculography and magnetic resonance imaging: a meta-analysis. *Eur J Nucl Med Mol Imaging.* 2003;30:851–858.
38. Gunning MG, Anagnostopoulos C, Davies G, Forbat SM, Ell PJ, Underwood SR. Gated technetium-99m-tetrofosmin SPECT and cine MRI to assess left ventricular contraction. *J Nucl Med.* 1997;38:438–442.
39. Tadamura E, Kudoh T, Motooka M, et al. Use of technetium-99m sestamibi ECG-gated single-photon emission tomography for the evaluation of left ventricular function following coronary artery bypass graft: comparison with three-dimensional magnetic resonance imaging. *Eur J Nucl Med.* 1999;26:705–712.
40. Wahba FF, Lamb HJ, Bax JJ, et al. Assessment of regional myocardial wall motion and thickening by gated 99m-Tc-tetrofosmin SPECT: a comparison with magnetic resonance imaging. *Nucl Med Commun.* 2001;22:663–671.
41. Chua T, Kiat H, Germano G, et al. Gated technetium-99m sestamibi for simultaneous assessment of stress myocardial perfusion, postexercise regional ventricular function and myocardial viability: correlation with echocardiography and rest thallium-201 scintigraphy. *J Am Coll Cardiol.* 1994;23:1107–1114.
42. Hoffman E, Huang S, Phelps M. Quantitation in positron emission computed tomography. 1. Effects of object size. *J Comput Assist Tomogr.* 1989;3:299–308.
43. Fukuchi K, Uehara T, Morozumi T, et al. Quantification of systolic count increase in technetium-99m-MIBI gated myocardial SPECT. *J Nucl Med.* 1997;38:1067–1073.
44. Maunoury C, Chen CC, Chua KB, Thompson CJ. Quantification of left ventricular function with thallium-201 and technetium-99m-sestamibi myocardial gated SPECT. *J Nucl Med.* 1997;38:958–961.
45. Ambrosio G, Betocchi S, Pace L, et al. Prolonged impairment of regional contractile function after resolution of exercise-induce angina: evidence of myocardial stunning in patients with coronary artery disease. *Circulation.* 1996;94:2455–2466.
46. Paul AK, Hasegawa S, Yoshioka J, et al. Exercise-induced stunning continues for at least one hour: evaluation with quantitative gated single-photon emission tomography. *Eur J Nucl Med.* 1999;26:410–415.
47. Paul AK, Hasegawa S, Yoshioka J, Mu X, Maruyama K, Kusuoka H, Nishimura T. Characteristics of regional myocardial stunning after exercise in gated myocardial SPECT. *J Nucl Cardiol.* 2002;9:388–394.
48. Mazzanti M, Germano G, Kiat H, Friedman J, Berman DS. Fast technetium 99m-labeled sestamibi gated single-photon emission computed tomography for evaluation of myocardial function. *J Nucl Cardiol.* 1996;3:143–149.
49. Yoshinaga K, Morita K, Yamada S, et al. Low-dose dobutamine electrocardiograph-gated myocardial SPECT for identifying viable myocardium: comparison with dobutamine stress echocardiography and PET. *J Nucl Med.* 2001;42:838–844.
50. Nakajima K, Higuchi T, Taki J, Kwano M, Tonami N. Accuracy of ventricular volume and ejection fraction measured by gated myocardial perfusion SPECT: comparison of 4 software programs. *J Nucl Med.* 2001;42:1571–1578.
51. Nichols K, Santana CA, Folks R, et al. Comparison between ECTb and QGS for assessment of left ventricular function from gated myocardial perfusion SPECT. *J Nucl Cardiol.* 2002;9:285–293.
52. Lum DP, Coel MN. Comparison of automatic quantification software for the measurement of ventricular volume and ejection fraction in gated myocardial perfusion SPECT. *Nucl Med Commun*. 2003;24:259–266.
53. Kikkawa M, Nakamura T, Sakamoto K, et al. Assessment of left ventricular diastolic function from quantitative electrocardiographic-gated ^{99m}Tc-tetrofosmin myocardial SPET. *Eur J Nucl Med.* 2001;28:593–601.
54. Maruyama K, Hasegawa S, Nakatani D, et al. Left ventricular mass index measured by quantitative gated myocardial SPECT with ^{99m}Tc-tetrofosmin: a comparison with echocardiography. *Ann Nucl Med.* 2003;17:31–39.
55. Akinboboye O, Germano G, Idris O, et al. Left ventricular mass measured by myocardial perfusion gated SPECT: relation to three-dimensional echocardiography. *Clin Nucl Med.* 2003;28:392–397.
56. Paul AK, Kusuoka H, Hasegawa S, Yonezawa T, Makikawa M, Nishimura T. Prolonged diastolic dysfunction following exercise-induced ischemia: a gated myocardial perfusion SPECT study. *Nucl Med Commun.* 2002;23:1129–1136.
57. Nakajima K, Taki J, Kawano M, et al. Diastolic dysfunction in patients with systemic sclerosis detected by gated myocardial perfusion SPECT: an early sign of cardiac involvement. *J Nucl Med.* 2001;42:183–188.
58. Sharir T, Berman DS, Waechter PB, et al. Quantitative analysis of regional motion and thickening by gated myocardial perfusion SPECT: normal heterogeneity and criteria for abnormality. *J Nucl Med.* 2001;42:1630–1638.
59. De Bondt P, Van de Wiele C, De Sutter J, De Winter F, De Backer G, Dierckx RA. Age- and gender-specific differences in left ventricular cardiac function and volumes determined by gated SPET. *Eur J Nucl Med.* 2001;28:620–624.
60. Rozanski A, Nichols K, Yao SS, Malholtra S, Cohen R, DePuey EG. Development and application of normal limits for left ventricular ejection fraction and volume measurements from ^{99m}Tc-sestamibi myocardial perfusion gated SPECT. *J Nucl Med.* 2000;41:1445–1450.
61. Manrique A, Faraggi M, Vera P, et al. ^{201}Tl and ^{99m}Tc-MIBI gated SPECT in patients with large perfusion defects and left ventricular dysfunction: comparison with equilibrium radionuclide angiography. *J Nucl Med.* 1999;40:805–809.
62. Nakajima K, Taki J, Higuchi T, et al. Gated SPET quantification of small hearts: mathematical simulation and clinical application. *Eur J Nucl Med.* 2000;27:1372–1379.
63. Constantine G, Shan K, Flamm SD, Sivananthan MU. Role of MRI in clinical cardiology. *Lancet.* 2004;363:2162–2171.
64. Mansoor MR, Heller GV. Gated SPECT imaging. *Semin Nucl Med.* 1999;29:271–278.
65. Bavelaar-Croon CD, Pawels EK, van der Wall EE. Gated single-photon emission computed tomographic myocardial imaging: a new tool in clinical cardiology. *Am Heart J.* 2001;141:383–390.
66. Go V, Bhatt MR, Hendel RC. The diagnostic and prognostic value of ECG-gated SPECT myocardial perfusion imaging. *J Nucl Med.* 2004;45:912–921.
67. Emmett L, Iwanochko RM, Freeman MR, Barolet A, Lee DS, Husain M. Reversible regional wall motion abnormalities on exercise technetium-99m-gated cardiac single photon emission computed tomography predict high-grade angiographic stenoses. *J Am Coll Cardiol.* 2002;39:991–998.
68. Saman P, Parson A, Lahiri N, et al. The prognostic value of a normal Tc-99m sestamibi SPECT study in suspected coronary artery disease. *J Nucl Cardiol.* 1999;6:252–256.
69. Danias PG, Ahlberg AW, Clark BA, et al. Combined assessment of myocardial perfusion and left ventricular function with exercise technetium-99m sestamibi gated single-photon emission computed tomography can differentiate between ischemic and nonischemic dilated cardiomyopathy. *Am J Cardiol.* 1998;82:1253–1258.
70. Smanio PE, Watson DD, Segalla DL, Vinson EL, Smith WH, Beller GA. Value of gating of technetium-99m sestamibi single-photon emission computed tomographic imaging. *J Am Coll Cardiol.* 1997;30:1687–1692.
71. Wahba FF, Baevelaar-Croon CD, Baur LH, et al. Detection of regional wall motion after sustained myocardial infarction by gated ^{99m}Tc-tetrofosmin SPECT: a comparison with echocardiography. *Nucl Med Commun.* 2001;22:175–182.
72. Kubo S, Tadamura E, Kudoh T, et al. Assessment of the effect of revascularization early after CABG using ECG-gated perfusion single-photon emission tomography. *Eur J Nucl Med.* 2001;28:230–239.